Towards Long-Distance Atom-Photon Entanglement

W. Rosenfeld,[1] F. Hocke,[1] F. Henkel,[1] M. Krug,[1] J. Volz,[1] M. Weber,[1,*] and H. Weinfurter[1,2]

[1]*Fakultät für Physik, Ludwig-Maximilians-Universität München, D-80799 München, Germany*
[2]*Max-Planck-Institut für Quantenoptik, 85748 Garching, Germany*
(Received 8 August 2008; published 31 December 2008)

We report the observation of entanglement between a single trapped atom and a single photon at remote locations. The degree of coherence of the entangled atom-photon pair is verified via appropriate local correlation measurements, after communicating the photon via an optical fiber link of 300 m length to a receiver 3.5 m apart. In addition, we measured the temporal evolution of the atomic density matrix after projecting the atom via a state measurement of the photon onto several well-defined spin states. We find that the state of the single atom dephases on a time scale of 150 μs, which represents an important step towards long-distance quantum networking with individual neutral atoms.

Entanglement between light and matter [1–4] plays an outstanding role in long-distance quantum communication, allowing efficient distribution of quantum information over, in principle, arbitrary large distances. By interfacing matter-based quantum processors and photonic communication channels, light-matter entanglement is regarded as a fundamental building block for future applications such as the quantum repeater [5] and quantum networks. In addition, this new kind of entanglement would allow, e.g., quantum teleportation [6] of quantum states of light onto matter [4,7] as well as the heralded generation of entanglement between quantum memories [8] via entanglement swapping [9]. Light-matter entanglement is thus not only crucial for long range quantum communication but forms the basis for a first loophole-free test of Bell's inequality with a pair of entangled atoms at remote locations [3,10].

So far, three different approaches entangling light and matter have been pursued. The spontaneous decay in a lambda-type transition of a single trapped atom or ion enables one to entangle the internal degree of freedom of the emitted photon with the spin state of the atom [1,3]. Experiments in this direction recently achieved the observation of entanglement between two individually trapped ions [8], the remote preparation of an atomic quantum memory [11], and the realization of a single-atom single-photon quantum interface based on optical high-Q cavities [12]. Other approaches are based on entanglement between coherently scattered photons and collective spin excitations in atomic ensembles [2,7,13] and entanglement between continuous variables of light and matter [4,14].

The relevance of light-matter entanglement for quantum networking arises from the fact that it establishes non-classical correlations between a localized matter-based quantum memory and an optical carrier of quantum information which can easily be sent to a distant location. Together with appropriate quantum communication protocols like quantum teleportation, this allows to map photonic quantum information into quantum memories, to

buffer quantum information, and to reconvert it later on again to photonic quantum carriers. In this context, decoherence of the photonic quantum channel, as well as, decoherence of the matter-based quantum memory are important figures of merit setting a limit how far quantum information can be distributed or how long this information can be stored, respectively. Therefore, the ability to generate and preserve light-matter entanglement over large distances [15] opens the possibility for long-distance distribution of quantum information [16].

In this Letter, we report the first direct observation of entanglement between the internal state of a single trapped ^{87}Rb atom and the polarization state of a single photon which has passed 300 m optical fiber. This is achieved by actively stabilizing both the birefringence of the optical fiber link, as well as, ambient magnetic fields in order to minimize dephasing of the atomic memory qubit, stored in the atomic ground state $5^2S_{1/2}$, $F = 1$, $m_F = \pm 1$. Detailed coherence measurements of the atomic qubit show that photonic quantum information can be stored for about 150 μs.

In our experiment, entanglement between the spin of a single optically trapped ^{87}Rb atom and the polarization of a photon is generated in the spontaneous emission process in a lambda-type transition [3], resulting in the maximally entangled atom-photon state

$$|\Psi\rangle = \frac{1}{\sqrt{2}}(|1, -1\rangle|\sigma^+\rangle + |1, +1\rangle|\sigma^-\rangle). \quad (1)$$

Here the two circular polarization states $\{|\sigma^+\rangle, |\sigma^-\rangle\}$ of the photon define the photonic qubit, and the angular momentum states $\{|F = 1, m_F = -1\rangle := |\downarrow\rangle_z$, $|F = 1, m_F = +1\rangle := |\uparrow\rangle_z\}$ the atomic qubit, respectively. While the atom is spatially localized in the optical dipole trap, the emitted photon is coupled into a single-mode optical fiber of 300 m length and guided to a separate optical breadboard at a distance of 3.5 m within the same lab where the polarization analysis is performed. To mea-

sure and compensate drifts of the fiber birefringence, reference laser pulses with two complementary polarizations $(V, +45°)$ are sent through the optical fiber (incorporating a fiber-based dynamic polarization controller) and the respective output polarizations are analyzed with a reference polarimeter [see Fig. 1(b)]. Based on the difference between input and output polarization, a software algorithm calculates new parameters for the dynamic polarization controller thereby optimizing the alignment. One such step takes 0.7 s, which is currently limited by the switching speed of the optomechanical shutters. These steps are repeated iteratively until input and output polarizations are identical within 99.9% [17]. Once the algorithm has compensated the fiber birefringence, typically after 10 steps, single photons from the atom are sent through the fiber. Under lab conditions, it was sufficient to repeat this algorithm every 10 min. To verify atom-photon entanglement, the internal atomic spin state is measured locally in two complementary measurement bases σ_x and $\sigma_y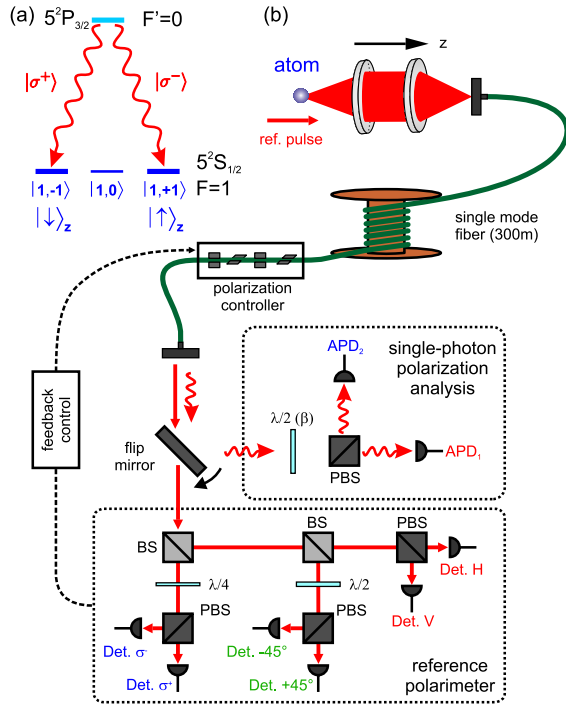$ with the help of a stimulated-Raman-adiabatic-passage technique [3,18] and correlated with the polarization analysis of the photon. The bare photon detection efficiency typically is 1.2×10^{-3}, including coupling losses into the single-mode optical fiber and the limited quantum efficiency of the single-photon detectors. Together with transmission losses in the optical fiber and coupling losses of the dynamic polarization controller, this results in the total detection efficiency of 0.6×10^{-3}. The final event rate is 15 min^{-1}, which is mainly caused by frequent reloading of the dipole trap after 50% of the atomic state measurements [3]. For the analysis of entanglement, we determined the probability of detecting the atomic qubit in $|\downarrow\rangle_x$ and $|\downarrow\rangle_y$ conditioned on the projection of the photon onto the states $1/\sqrt{2}(|\sigma^+\rangle \pm e^{2i\beta}|\sigma^-\rangle)$ [see Figs. 2(a) and 2(b)]. For $\beta = 0°$ the Si avalanche photo-diodes APD$_1$ and APD$_2$ analyze the photonic qubit in the eigenstates $|H\rangle := 1/\sqrt{2}(|\sigma^+\rangle + |\sigma^-\rangle)$ and $|V\rangle := 1/\sqrt{2}(|\sigma^+\rangle - |\sigma^-\rangle)$ of $\hat{\sigma}_x$, whereas for $\beta = 45°$ APD$_1$ and APD$_2$ project onto the eigenstates $|+45°\rangle := 1/\sqrt{2}(|\sigma^+\rangle - i|\sigma^-\rangle)$ and $|-45°\rangle := 1/\sqrt{2}(|\sigma^+\rangle + i|\sigma^-\rangle)$ of $\hat{\sigma}_y$. As expected, if a $|V\rangle$-polarized photon is detected, the atom is found with high probability in the corresponding state $|\downarrow\rangle_x$, whereas if a $|H\rangle$-polarized photon is registered the atom is with low

FIG. 1 (color online). Schematic of long-distance atom-photon entanglement. (a) During the spontaneous decay of a single optically trapped ^{87}Rb atom on the transition $5^2P_{3/2}$, $F' = 0 \rightarrow 5^2S_{1/2}$, $F = 1$ the polarization of the emitted photon gets entangled with the final spin state of the atom. (b) The emitted photon is coupled into a single-mode optical fiber and communicated to a remote location where a polarization analysis is performed. To overcome thermally and mechanically induced fluctuations of the fiber birefringence, an active polarization compensation is used. Therefore reference laser pulses are sent through the optical fiber and the output polarizations are characterized in a reference polarimeter. With the help of a software algorithm and a dynamic polarization controller it is ensured that input and output polarizations are identical.
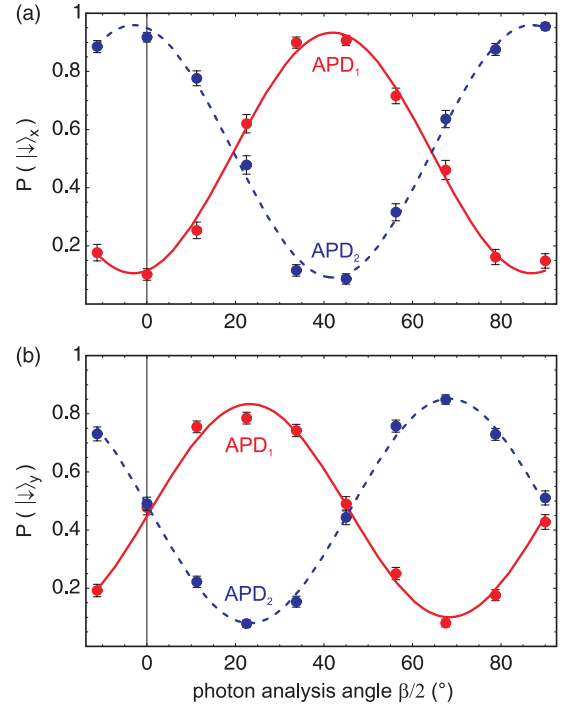

FIG. 2 (color online). Verification of atom-photon entanglement. Probability of detecting the atomic qubit in (a) $|\downarrow\rangle_x := 1/\sqrt{2}(|\uparrow\rangle_z - |\downarrow\rangle_z)$ and (b) $|\downarrow\rangle_y := 1/\sqrt{2}(|\uparrow\rangle_z - i|\downarrow\rangle_z)$ conditioned on the detection of the photon in detector APD$_1$ or APD$_2$, where the photonic qubit is projected onto the states $1/\sqrt{2}(|\sigma^+\rangle \pm e^{2i\beta}|\sigma^-\rangle)$. The phase β can be set with a rotatable $\lambda/2$ wave plate in front of a polarizing beam splitter (PBS). For $\beta = 0°$, respectively, $\beta/2 = 22.5°$ the photon is analyzed in the complementary measurement bases σ_x and σ_y.

probability in the state $|\downarrow\rangle_x$. Observing similar correlations in the complementary σ_y basis of the atom [see Fig. 2(b)] confirms that the atom-photon pair is in the entangled state $|\Psi\rangle$ [see Eq. (1)]. To determine the degree of entanglement, sinusoidal functions were fitted onto the measured atom-photon correlation data. From the fits we infer a visibility of $V_{\sigma_x} = 0.85 \pm 0.03$ for the analysis of the atomic qubit in σ_x and $V_{\sigma_y} = 0.75 \pm 0.03$ for σ_y, respectively. The limited visibility of the atom-photon correlations is caused mainly by errors in the atomic state detection (7%), accidental photon detection events due to dark counts of the single-photon detectors (3%), errors in the preparation of the initial state (1%), polarization drifts in the optical fiber during successive stabilization sequences of the dynamic polarization compensation (1%), and residual shot-to-shot dephasing of the atomic qubit due to fluctuations of the ambient magnetic field. For the significantly reduced visibility in the atomic σ_y basis we suppose residual magnetic fields along the x axis, which lead to Larmor precession into the additional Zeeman sublevel $m_F = 0$ of the $5^2S_{1/2}$, $F = 1$ hyperfine ground level [19]. To estimate the atom-photon entanglement fidelity F_{at-ph}, we assume that errors in the atomic and photonic state detection are isotropic in all three complementary measurement bases (white noise). Herewith, we derive a minimum fidelity F_{at-ph} of 0.85 ± 0.02.

For future applications in long-distance quantum communication, absorption losses and depolarization of the photonic qubit in optical fibers are important figures of merit, thereby limiting the distance over which quantum information can be distributed. Another crucial criterion for these applications will be the ability to store quantum information in quantum memories, which show long coherence times. So far, for quantum memories based on Zeeman qubits of neutral atoms, experimental coherence times of several 10 μs have been demonstrated [7,15]. In principle, clock-state quantum memories can have much longer coherence times [20], yet, manipulation of the corresponding light-matter entanglement is far less practical.

In order to carefully distinguish between photonic and atomic decoherence, we characterized the coherence properties of the atomic quantum memory by measuring the precession of the atomic spin in a magnetic field. This is achieved via quantum state tomography of the atomic ground level $5^2S_{1/2}$, $F = 1$, reconstruction of the respective density matrix $\rho = r|\chi\rangle\langle\chi| + (1 - r)\hat{1}/3$ [19], and determination of the corresponding purity parameter r. In contrast to the fidelity, $F = \langle\Phi|\rho|\Phi\rangle$, which is the overlap between the measured density matrix ρ and a pure target state $|\Phi\rangle$, the purity parameter, here $r = \sqrt{1/2[3\mathrm{tr}(\rho^2) - 1]}$, is related to the coherent fraction of the density matrix with respect to the *closest* pure state $|\chi\rangle$ (which is in general unknown). Therefore r is ideally suited to quantify decoherence effects of our atomic quantum memory.

In our spin-precession experiments, the 300 m optical fiber of the first experiment is replaced by a 5 m one, leading to a negligible time delay of 25 ns between the preparation of the entangled atom-photon pair and the initialization of the atomic spin state via a projective polarization measurement of the photon. The magnetic bias field is controlled via additional Helmholtz coils and an active feedback loop with an accuracy of $|B| < 2$ mG. After the atomic spin has freely evolved in the magnetic field for defined time periods, tomography of the final atomic spin state was performed by measuring populations of the atomic eigenstates of the Pauli spin operators $\hat{\sigma}_x$, $\hat{\sigma}_y$, and $\hat{\sigma}_z$ [11]. In the case where a small magnetic guiding field of 5.5 mG is applied along the quantization axis z, we observe the expected Larmor precession of a spin-1/2 atom (see Fig. 3), with a $1/e$ dephasing time of 150 μs. In the general case where a magnetic guiding field is not along the z axis or in the case where no guiding field is applied, the atom can press out of the qubit subspace $\{|1, -1\rangle, |1, +1\rangle\}$ into the $|F = 1, m_F = 0\rangle$ Zeeman state of the $5^2S_{1/2}$, $F = 1$ hyperfine ground level. Thus, for complete characterization of decoherence effects it is necessary to reconstruct the 3×3 spin-1 density matrix ρ. This is possible with certain constraints. Coherences between the states $|1, \pm1\rangle$ and $|1, 0\rangle$ cannot be measured with the present atomic state detection technique, as the applied stimulated-Raman-adiabatic-passage pulses analyze only the $\{|1, -1\rangle, |1, +1\rangle\}$ qubit subspace in a complete way [3,11]. However, the population in the $|1, 0\rangle$ state can be inferred as the population missing in the $\{|1, -1\rangle, |1, +1\rangle\}$ subspace. To reconstruct the density matrix ρ of the spin-1 state, we apply a worst-case assumption that there is no coherence between the $|1, 0\rangle$ state and the others, and set the corresponding components to 0. The resulting purity parameter r thus is a conservative lower bound on the effective coherence of the atomic state.

In a second measurement run, no guiding field is applied (corresponding to the situation of a magnetic zero field with an accuracy of ±2 mG) and dephasing of the atomic
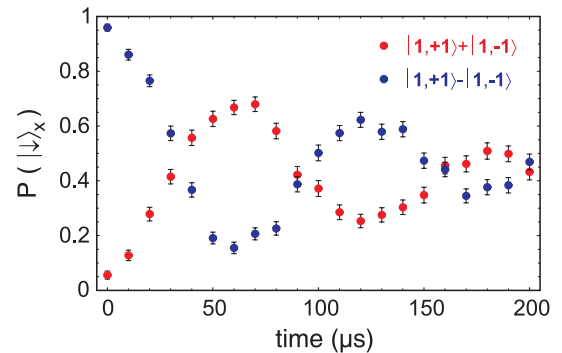

FIG. 3 (color online). Spin precession of the atomic states $\{|\uparrow\rangle_x := 1/\sqrt{2}(|\uparrow\rangle_z + |\downarrow\rangle_z), |\downarrow\rangle_x := 1/\sqrt{2}(|\uparrow\rangle_z - |\downarrow\rangle_z)\}$, as a guiding field of 5.5 mG is applied along the quantization axis z. After the temporal evolution the population P of the $|\downarrow\rangle_x$ state is measured.
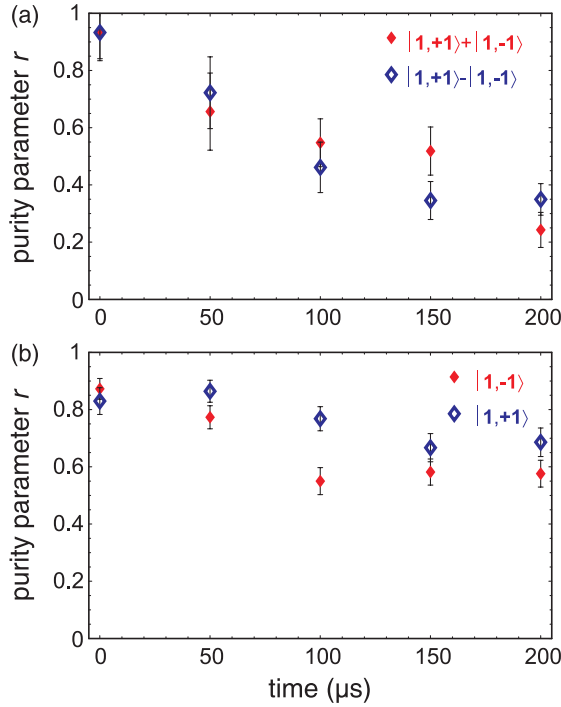
FIG. 4 (color online).   Temporal evolution of the lower bound of the purity parameter r as the atom is prepared initially in the states (a) $\{|\uparrow\rangle_x := 1/\sqrt{2}(|\uparrow\rangle_z + |\downarrow\rangle_z), |\downarrow\rangle_x := 1/\sqrt{2}(|\uparrow\rangle_z - |\downarrow\rangle_z)\}$, (b) $\{|\uparrow\rangle_z := |1, +1\rangle, |\downarrow\rangle_z := |1, -1\rangle\}$. Each measurement point results from a partial quantum state tomography of the spin-1 ground level $5^2S_{1/2}, F = 1$.

superposition states $1/\sqrt{2}(|1, -1\rangle \pm |1, +1\rangle)$ is analyzed by reconstruction of the minimal purity parameter r. Here we find transversal $1/e$ dephasing times of $T_2^* = 75..150\ \mu s$; see Fig. 4(a). For the states $|1, \pm 1\rangle$, see Fig. 4(b), the longitudinal dephasing times are estimated by extrapolation to be >0.5 ms. The faster dephasing of superposition states show that fluctuations, respectively, shot-to-shot noise of the effective magnetic field, are mainly along the quantization axis z. This effect is due to a small fraction of circularly polarized dipole-trap light (below 1%), which leads in combination with a finite atomic temperature of 150 μK to a position-dependent differential light shift [19].

In this Letter, we successfully demonstrated the generation and verification of entanglement between a single trapped neutral atom and single photon separated by 300 m optical fiber. Our implementation includes an active stabilization of ambient magnetic fields with an accuracy of $|B| < 2$ mG, resulting in a dephasing time of the atomic memory level $5^2S_{1/2}, F = 1$ of $\simeq 150\ \mu$s. Longer coherence times could be reached with higher accuracy of the polarization of the dipole-trap light, lower temperature of the trapped atom, and better stability of the magnetic field. Nevertheless, together with the implemented stable optical

fiber link, also the current setup should allow to entangle two optically trapped ^{87}Rb atoms at locations spatially separated by several 100 m, ready for future applications in long-distance quantum networking with neutral atoms and a loophole-free test of Bell's inequality [3].

*Corresponding author.
markus.weber@physik.uni-muenchen.de

[1] B. B. Blinov, D. L. Moehring, L.-M. Duan, and C. Monroe, Nature (London) **428**, 153 (2004).
[2] D. N. Matsukevich *et al.*, Phys. Rev. Lett. **95**, 040405 (2005).
[3] J. Volz, *et al.*, Phys. Rev. Lett. **96**, 030404 (2006).
[4] J. F. Sherson *et al.*, Nature (London) **443**, 557 (2006).
[5] H.-J. Briegel, W. Dür, J. I. Cirac, and P. Zoller, Phys. Rev. Lett. **81**, 5932 (1998).
[6] C. H. Bennett *et al.*, Phys. Rev. Lett. **70**, 1895 (1993); D. Bouwmeester *et al.*, Nature (London) **390**, 575 (1997); A. Furusawa *et al.*, Science **282**, 706 (1998).
[7] Y. A. Chen *et al.*, Nature Phys. **4**, 103 (2008).
[8] D. L. Moehring *et al.*, Nature (London) **449**, 68 (2007); D. N. Matsukevich, P. Maunz, D. L. Moehring, S. Olmschenk, and C. Monroe, Phys. Rev. Lett. **100**, 150404 (2008).
[9] M. Zukowski, A. Zeilinger, M. A. Horne, and A. K. Ekert, Phys. Rev. Lett. **71**, 4287 (1993).
[10] K. Saucke, Diploma thesis, University of Munich, 2002; C. Simon and W. T. M. Irvine, Phys. Rev. Lett. **91**, 110405 (2003).
[11] W. Rosenfeld, S. Berner, J. Volz, M. Weber, and H. Weinfurter, Phys. Rev. Lett. **98**, 050504 (2007).
[12] T. Wilk, S. C. Webster, A. Kuhn, and G. Rempe, Science **317**, 488 (2007); A. D. Boozer, A. Boca, R. Miller, T. E. Northup, and H. J. Kimble, Phys. Rev. Lett. **98**, 193601 (2007).
[13] C. W. Chou *et al.*, Nature (London) **438**, 828 (2005); D. N. Matsukevich *et al.*, Phys. Rev. Lett. **96**, 030405 (2006).
[14] B. Julsgaard, J. Sherson, J. I. Cirac, J. Fiurasek, and E. S. Polzik, Nature (London) **432**, 482 (2004).
[15] H. de Riedmatten *et al.*, Phys. Rev. Lett. **97**, 113603 (2006).
[16] C. Simon *et al.*, Phys. Rev. Lett. **98**, 190503 (2007); O. A. Collins, S. D. Jenkins, A. Kuzmich, and T. A. B. Kennedy, Phys. Rev. Lett. **98**, 060502 (2007).
[17] F. Hocke, Diploma thesis, University of Munich, 2007.
[18] F. Vewinger, M. Heinz, R. Garcia Fernandez, N. V. Vitanov, and K. Bergmann, Phys. Rev. Lett. **91**, 213001 (2003).
[19] W. Rosenfeld, Ph.D. thesis, University of Munich, 2008.
[20] S. Kuhr *et al.*, Phys. Rev. Lett. **91**, 213002 (2003); M. P. A. Jones *et al.*, Phys. Rev. A **75**, 040301(R) (2007).